

TrajPred: Trajectory-Conditioned Joint Embedding Prediction for Surgical Instrument-Tissue Interaction Recognition in Vision-Language Models

Jiajun Cheng, Xiaofan Yu, Subarna, Sainan Liu, Shan Lin

Abstract—Recognizing instruments’ interactions with tissues is essential for building context-aware AI assistants in robotic surgery. Vision-language models (VLMs) have opened a new avenue for surgical perception and achieved better generalization on a wide range of tasks compared to conventional task-specific deep learning approaches. However, their performance on instrument–tissue interaction recognition remains limited, largely due to two challenges: (1) Many models do not effectively leverage temporal information, (2) alignment between vision and text often misses fine-grained action details. To address these issues, we propose **TrajPred**, a framework that encodes instrument trajectories to incorporate temporal motion cues; and conditioned on these trajectories, introducing a predictor module to generate visual semantic embeddings that better capture fine-grained action details. We further incorporate prompt tuning and a verb-rephrasing technique to enable smooth adaptation to the Instrument-Tissue interaction recognition task. Extensive experiments on the public laparoscopic benchmark, CholecT50, show that our method improves both Average Precision and Top-K accuracy.

We also investigate whether visual embeddings of instrument-tissue interaction regions align better with the corresponding text by visualizing the cosine similarity between visual and textual embeddings. The visualization results indicate that the proposed method improves alignment between relevant visual and textual representations. Code is available at <https://github.com/jiajun344/TrajPred>.

I. INTRODUCTION

Robotic surgery has been widely adopted due to improved ergonomics, clinical outcomes, and reduced complication rates [8]. However, in hospitals, current robotic systems remain fully surgeon-operated, and surgical quality still depends heavily on surgeon experience, performance variability, and availability. These limitations have motivated increasing interest in robotic automation to achieve more consistent and reproducible performance [35], [26]. Recognizing Instrument-Tissue interactions is a critical component for enabling effective collaboration between robots and surgeons, allowing robots to understand and respond appropriately to surgeons’ actions. In the future, this capability can also guide robots in learning surgical skills from expert demonstrations.

Instrument-Tissue interaction recognition are typically formulated as surgical action triplets structured as (*instrument, verb, target*)[22]. Such triplet representations are also commonly used in general-domain action recognition tasks [7]. Traditional surgical triplet recognition methods are typically built on classifier-based architectures that predict the instrument, verb, and target separately using independent classification heads [21], [19], [11]. Although these approaches

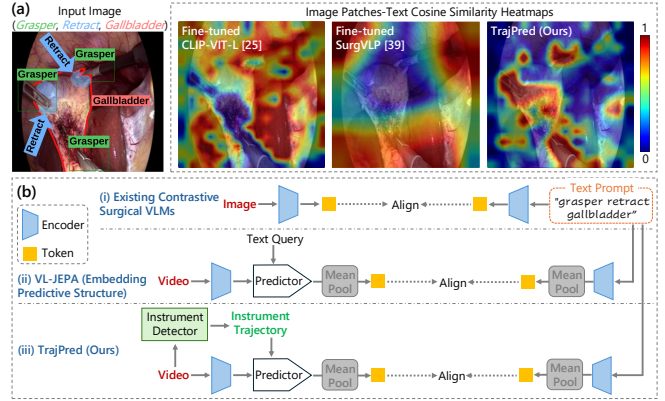


Fig. 1. (a) Cosine similarity heatmaps between embeddings of image patches and the text (e.g., “grasper retract gallbladder”). Two representative contrastive learning-based VLMs (CLIP-ViT-L [24] and SurgVLP [38]) exhibit high similarity between background patches and the text, whereas TrajPred (ours) produces embeddings that concentrate on the Instrument-Tissue interaction region. (b) Comparison of the architectures of (i) popular contrastive learning-based surgical VLMs, (ii) VL-JEPA[2], and (iii) TrajPred.

have improved performance on commonly used surgical action triplet datasets [22], classifier-based architectures rely on clearly labeled samples, learning decision boundaries tailored to predefined training categories. However, obtaining such detailed annotations is expensive, and models trained in this way often struggle to generalize to diverse real-world surgical settings where procedures may appear under different environments or conditions.

Recent progress in contrastive learning vision–language models (VLMs) offers a promising approach to addressing these generalization limitations. Unlike classifier-based architectures that learn to directly map images to predefined labels, VLMs learn representations by aligning visual features with textual descriptions in a shared embedding space [15], [24]. Pretrained on large-scale and diverse data, VLMs effectively bridge visual and natural language embeddings, this allows training to leverage audio captions from large publicly available surgical video databases online, reducing the labeling burden while learning semantic representations better generalize to the same surgical procedures under different environments and visual conditions. Building on this paradigm, several works [38], [36], [37], [40] have leveraged large-scale surgical video datasets to develop VLMs tailored to the surgical domain, demonstrating the potential of VLMs across various surgical perception tasks. However, existing studies on surgical VLMs indicate that their performance on surgical action triplet recognition remains limited [25], [40].

Two key limitations hinder the performance of VLMs for Instrument-Tissue interaction recognition

(1) **Limited Use of Detailed Temporal Information Across Frames.** Many existing surgical contrastive learning VLM approaches [27], [38], [36], [37], [40] rely on single-frame inputs paired with text captions during training. Similar to traditional methods, many Instrument-Tissue interaction recognition models also operate on single frames [21], [11]. Inferring surgical actions from a single frame is inherently ambiguous. While certain actions, such as grasping (Fig. 2(a)), may be inferred from static visual cues, many others require information across multiple frames to observe motion patterns (Fig. 2(b)). Although single-image models may achieve reasonable performance because certain instruments are strongly associated with specific actions, this reliance can limit the model’s ability to understand how instruments actually perform different actions. As a result, such approaches are less reliable for intraoperative applications, where accurate, robust, and explainable recognition of ongoing surgical actions is critical.

(2) **Suppression of Details in Contrastive Learning.** As current visual encoders commonly split images into multiple image patches, most surgical VLMs are trained using contrastive learning that aligns visual features aggregated from the entire image with the corresponding text (Fig. 1(b)(i)). While effective for global semantics, this strategy often suppresses fine-grained spatial details [6], [34], but in a surgical setting, pooled visual features may contain substantial background information, with only a small portion relevant to the text. Fig. 1(a) shows an example comparing image patch-text embedding cosine similarity heatmaps between two representative contrastive learning-based VLMs (surgical-pretrained SurgVLP [38] and the general pretrained CLIP [24]) and our TrajPred, where existing models highlight background whereas our model focuses on the Instrument-Tissue interaction region. Recent surgical VLM benchmark studies [5] have also highlighted the loss of fine-grained details and raised concerns regarding the reliability of current VLMs for surgical decision support. Although recent work such as [6], [34] proposes object-level alignment by aligning image patches fall within bounding boxes of target objects to corresponding text tokens, this approach is not directly applicable to our task, as Instrument-Tissue interaction involves action recognition and it is difficult or even impractical to define a bounding box for the action.

To mitigate these two limitations, we propose TrajPred, a trajectory-conditioned joint embedding prediction framework for vision–language. To better leverage temporal information, we use video clips as input and explicitly encode instrument trajectories to support action triplet recognition (Fig. 1(b)(iii)). To mitigate detail suppression in contrastive learning, inspired by VL-JEPA [2] (Fig. 1(b)(ii); a VLM achieves state-of-the-art video understanding), we adapt its trainable predictor module to predict semantic embeddings conditioned on trajectory tokens, enabling better capture of fine-grained action details (Fig. 1(b)(iii)). Finally, fine-tuning VLMs often degrades their generalization ability [4], [42].

To mitigate this issue, we reformulate surgical verbs into simplified but detailed english sentences and apply CoOp-style prompt tuning [43] to retain semantic priors in the pre-trained text encoder for smooth Instrument-Tissue interaction recognition task adaptation. In summary, our contributions are as follows:

- We reformulate Instrument-Tissue interaction recognition as an embedding prediction problem, replacing contrastive learning alignment with a semantic embedding predictive framework for to capture fine-grained action details.
- We extract instrument trajectory tokens to condition the embedding prediction, capturing their temporal motion cues across frames for better action recognition.
- We reformulate surgical verbs into descriptive prompts and apply prompt tuning to improve generalization capability.
- We conduct extensive experiments to demonstrate that TrajPred improves action triplet recognition performance and generalization while enhancing alignment between visual and text embeddings.

II. RELATED WORK

a) Instrument-Tissue Interaction recognition: In the surgical domain, the Instrument-Tissue interaction recognition task aims to predict a structured representation of surgical activity in the form of an (instrument, verb, target) triplet [22], e.g., (scissors, cut, tissue), indicating which instrument performs which action on which target. Traditional approaches typically adopt classifier-based frameworks that use separate classification heads for instrument, verb, and target [21], [28], [19], [11]. However, such methods rely heavily on expensive well-labeled datasets and often struggle to generalize to the same surgical procedures performed under different environments or conditions.

b) Surgical VLMs: VLMs have recently advanced surgical scene understanding. Prior surgical VLMs, including SurgVLP [38], HecVLP [36], and PeskaVLP [37], leverage large-scale surgical video corpora for contrastive learning pretraining and domain adaptation, incorporating hierarchical supervision and LLM-augmented knowledge. Beyond image–caption contrastive learning, recent works [23], [12], [31], [16] pretrain surgical video–language models by constructing large-scale surgical lecture video datasets collected online, adopting either contrastive learning objectives or autoregressive LLM-based training paradigms. Overall, current surgical VLM research primarily emphasizes dataset curation, focusing on the scale and quality of video–caption pairs. However, existing methods often overlook whether visual and textual representation are truly aligned in detailed-level, as shown in Fig. 1(a), which is crucial for AI trustworthiness, particularly in the medical domain [5]. In this paper, we show that our TrajPred framework avoids overlooking detailed action recognition and achieves better visual feature–text embedding alignment.

c) Temporal information in Surgery: Temporal information has been widely used in surgical data analysis tasks,

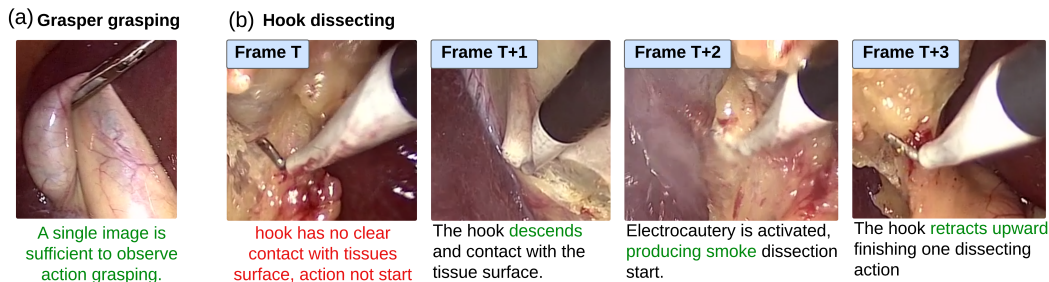


Fig. 2. Comparison between frames of the actions (a)“Grasper grasp” and (b)“Hook dissect”.

such as semantic segmentation [9], [18], phase recognition [10], [20], and surgical action triplet recognition [28]. Most of these methods are still trained with a small dataset and focus on specific tasks without good generalization capability. In the VLM domain, most approaches on surgical VLM training with temporal information mainly rely on large-scale publicly available surgical video clips, pairing audio-transcribed text with video clips for VLM training [23], [12], [31], [16] without explicitly care about fine-grained details in surgical actions. In *TrajPred*, we address these issues by explicitly encoding detailed instrument trajectories to better capture fine-grained visual details.

d) Fine-grained details alignment in VLMs: Recent works extend contrastive VLM alignment from global image features to finer spatial regions. Some methods use object detectors to align visual features from object regions with corresponding text tokens [3], [39], [14], while others apply soft region grouping to form coherent feature clusters and perform region–text contrastive learning without explicit localization [27], [44], [33]. More recent approaches explore automatic object alignment, e.g., using SAM to extract object regions followed by pretrained contrastive models for object–sentence matching [6]. Although these methods improve object-level alignment and model performance, surgical action understanding involves temporal relationships between objects [17], [32] rather than merely forcing features within regions of objects in the video to align with their corresponding object texts To address this, *TrajPred* leverages all visual features and employs a VL-JEPA-style predictor conditioned on trajectory information to learn action-aware semantic embeddings instead of relying on object-level alignment.

III. PROPOSED METHODS

The proposed *TrajPred* framework reformulates conventional contrastive VLM training into an embedding prediction paradigm for the Instrument–Tissue interaction recognition task. Specifically, we replace standard contrastive alignment with the VL-JEPA-inspired predictive embedding structure [2], and further extend it with a trajectory encoding module to explicitly model instrument motion. Surgical action recognition task is commonly formulated as instrument–verb–target triplet recognition [22], e.g., (*hook, dissect, gallbladder*), the triplet explicitly captures tool–tissue interactions. Similar structured representations are also widely used in general-domain egocentric action datasets [7]. We first describe the overall predictor

architecture of VL-JEPA, which our method builds upon, in Section III-A, followed by how our *TrajPred* method integrates trajectory tokens in Section III-B and text encoder design and verb rephrasing method in Section III-B.1 and III-B.2. Finally, we present the optimization and training objective in Section III-C.

A. VL-JEPA Structure

VL-JEPA [2] consists of three components: (i) a frozen visual encoder, (ii) a predictor module, and (iii) a text encoder.

a) Visual Encoder: Given a video clip $\mathbf{V} = \{I_t\}_{t=1}^T$, The visual encoder partitions it into spatio-temporal tubelet tokens and produces $\mathbf{Z}_v \in \mathbb{R}^{N_v \times D_v}$. The visual encoder remains frozen during training.

b) Text Encoder: The text encoder maps a natural language query into a semantic embedding $\mathbf{z}_t \in \mathbb{R}^{D_t}$, which serves as the alignment target in the joint embedding space. The text encoder is trainable during training.

c) Predictor: The predictor takes all visual tokens representation \mathbf{Z}_v and query tokens to predict final target embedding, unlike contrastive learning methods that rely on a single [CLS] token that summarize entire clip as the final visual embedding. The final embedding $h \in \mathbb{R}^{D_t}$ is obtained via mean pooling over the predictor outputs.

B. *TrajPred* Framework

While VL-JEPA demonstrates strong performance in video understanding tasks through embedding prediction and predictor module leverage all visual encoder outputs tokens [2], surgical videos often contain significant spurious motion (e.g., camera movement), which may still lead the predictor to attend to spurious cues. We therefore introduce a trajectory token encoding pathway to explicitly guide learning toward informative instrument dynamics. Inspired by [41], we construct a single trajectory token for each detected instrument k in the clip. The method consists of two streams: (1) an appearance stream that captures the instrument’s visual features across frames, and (2) a position stream that captures the instrument’s trajectory information over time, as illustrated in Fig. 3. We first employ a Fast R-CNN–based detector [13] trained on surgical instrument data to extract bounding boxes for each instrument in every frame, the bounding boxes serve as positional information for constructing trajectory tokens, as instrument movements—toward, away, or in different directions—are reflected in the changes of their bounding box coordinates. Notably, our framework is detector-agnostic,

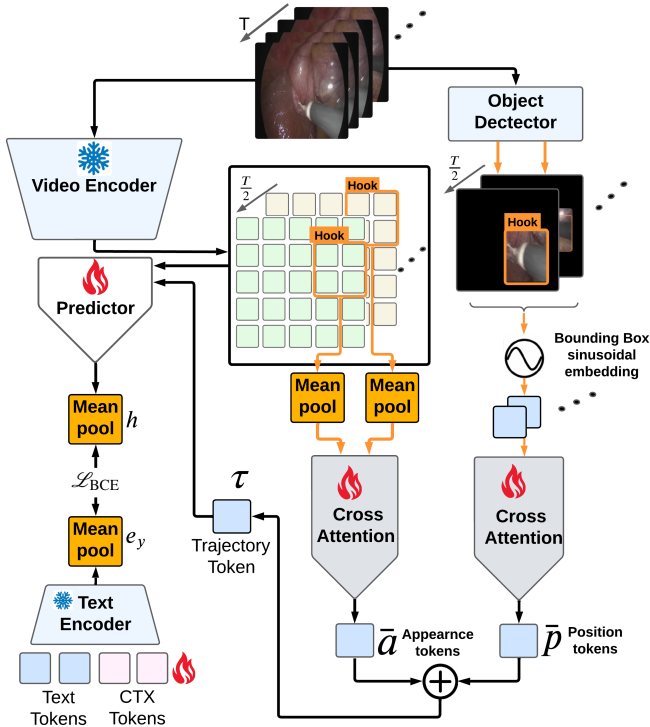


Fig. 3. Overview of TrajPred pipeline. Video clips are processed by both the video encoder and an object detector. Visual tokens within detector-predicted bounding boxes are mean-pooled and combined with bounding box coordinate embeddings through element-wise addition, forming trajectory tokens that are subsequently encoded via cross-attention. The resulting trajectory tokens are jointly fed with video encoder tokens into the predictor.

any object detection or instance segmentation model capable of localizing surgical instruments can be used to obtain the bounding box coordinates. Let $\{b_t^{(k)}\}_{t=1}^{T_k}$ denote the bounding box coordinates of instrument k over T_k frames.

a) *Appearance stream*: For each frame t , we mean-pool tubelet tokens \mathbf{Z}_v within the bounding box $b_t^{(k)}$ to obtain a per-frame appearance feature $a_t^{(k)} \in \mathbb{R}^{D_v}$. The temporal sequence $\{a_t^{(k)}\}_{t=1}^{T_k}$ is aggregated by a lightweight cross-attention pooling module (two layers, eight heads) with a single learnable query token that attends to the sequence as keys and values, producing $\bar{a}^{(k)} = \text{CrossAttnPool}(\{a_t^{(k)}\}_{t=1}^{T_k})$, where $\bar{a}^{(k)} \in \mathbb{R}^{D_v}$ summarizes the temporal appearance of instrument k . The position stream uses the same architecture with a separate learnable query.

b) *Position stream*: The bounding box coordinates $b_t^{(k)} \in \mathbb{R}^4$ are mapped into D_v -dimensional sinusoidal positional embeddings $p_t^{(k)} \in \mathbb{R}^{D_v}$ using fixed sine and cosine functions at multiple frequencies, encoding the spatial location of each instrument at each timestep. The temporal sequence $\{p_t^{(k)}\}_{t=1}^{T_k}$ is then compressed by a separate same cross-attention pooling module as appearances stream with its own learnable query token into a single position token $\bar{p}^{(k)} \in \mathbb{R}^{D_v}$.

c) *Fusion*: The final trajectory token for instrument k is defined as $\tau^{(k)} = \bar{a}^{(k)} + \bar{p}^{(k)} \in \mathbb{R}^{D_v}$. Element-wise summation is used to ensure each instrument trajectory is represented by a single token to ensure the token count is within a reasonable range. The trajectory tokens $\{\tau^{(k)}\}_{k=1}^K$ are concatenated with the video tubelet tokens \mathbf{Z}_v to form

TABLE I
VERB REPHRASING USED FOR PROMPT CONSTRUCTION.

Verb	Rephrased Phrase
grasp	holding and gripping
retract	pulling aside
dissect	separating by cutting
coagulate	stopping bleeding by heating
clip	clipping closed
cut	cutting through
aspirate	sucking fluid from
irrigate	washing with liquid
pack	pressing material onto
null_verb	not acting

$\mathbf{Z}_{\text{aug}} = [\mathbf{Z}_v; \tau^{(1)}, \dots, \tau^{(K)}]$, where K denotes the number of valid instrument trajectories. The augmented sequence \mathbf{Z}_{aug} is then fed into the predictor.

1) *Text Encoder Tuning*: We follow the same text encoder design as VL-JEPA [2], obtaining full surgical action triplet embeddings using a pretrained Embedding Gemma encoder [30]. Instead of fine-tuning the entire text encoder, we adopt CoOp-style prompt tuning [43] for better generalization capability. This approach optimizes a small set of learnable context tokens while keeping the backbone model parameters frozen, thereby retaining more of the pretrained knowledge. We prepend M learnable context tokens $\{c_m\}_{m=1}^M$ to the tokenized text sequence $\{y_j\}_{j=1}^L$, forming the input $[c_1, \dots, c_M, y_1, \dots, y_L]$. Only the context tokens are trainable, while the Gemma encoder weights remain fixed. The encoder outputs are mean pooled final text embedding $e_y \in \mathbb{R}^{D_t}$.

2) *Verb Phrase*: To mitigate the domain gap between surgical-specific verbs and the general-language vocabulary learned during large-scale pretraining, we replace the original verb labels with more descriptive natural language phrases in both training and evaluation. The complete verb-to-phrase mapping is provided in Table I, and all TrajPred results are reported using this formulation.

C. Training Optimization

Let $h_i \in \mathbb{R}^{D_t}$ and $e_c \in \mathbb{R}^{D_t}$ denote the predictor output and text embedding for sample i and class c , respectively. We compute cosine similarity logits $s_{i,c}$ and optimize a multi-label binary cross-entropy loss [43]:

$$\mathcal{L}_{\text{BCE}} = \frac{1}{NC} \sum_{i,c} \left[-y_{i,c} \log \sigma(s_{i,c}) - (1-y_{i,c}) \log (1-\sigma(s_{i,c})) \right],$$

where $y_{i,c} \in \{0, 1\}$ is the ground-truth label and $\sigma(\cdot)$ is the sigmoid function.

IV. EXPERIMENTS

A. Dataset and Metrics

In this paper, we conduct experiments on the CholecT50 dataset[22], a surgical action triplet recognition benchmark consisting of 50 laparoscopic cholecystectomy videos sampled from CholecT80 video dataset [29] and annotated in 1FPS with 100 action triplet classes in the form (instrument, verb, target). The dataset contains 100.9K video frames and over 151K triplet instances, constructed from 6 instrument

classes, 10 verb classes, and 15 target classes. For reproducibility, we follow the official Rendezvous (RDV) split for training and testing. Performance is evaluated using two metrics:

a) *Average precision*: We report the Average Precision (AP) metrics following the official evaluation protocol introduced in CholecT50 dataset [22], including triplet-level AP_{IVT} as well as component-level AP for instrument (AP_I), verb (AP_V), and target (AP_T).

b) *Top-K accuracy*: We report Top-K accuracy to evaluate the ranking quality of triplet predictions. For each sample i , the model computes cosine similarity scores with all C triplet prompts, producing a score vector $p_i \in \mathbb{R}^C$. Let $\text{TopK}(p_i)$ denote the top-K highest-scoring triplets and GT_i the set of ground-truth triplets. The Top-K accuracy over N test samples is defined as $\text{Top@K} = \frac{1}{N} \sum_{i=1}^N \frac{|\text{TopK}(p_i) \cap \text{GT}_i|}{|\text{GT}_i|}$. This measures the proportion of ground-truth triplets retrieved within the top-K predictions. We additionally report $\text{TOP@}(K=|\text{GT}|)$, where $K_i = |\text{GT}_i|$ is set to the number of ground-truth triplets for each sample and the final score is averaged over all samples.

B. Evaluation Strategy

a) *Baseline*: We compare TrajPred with seven baselines trained under the same CholecT50 RDV split, including CLIP [24], CLIP-GOAL [6], and surgical pretrained VLMs such as SurgVLP [38], HecVL [36], and PeskaVLP [37]. We also implement and follow the same setup as VL-JEPA [2] with both image-based and video-based variants using the text query “What is the action shown?”

b) *Experiment setting*: We evaluate Performance under two settings. (1) We follow the CholecT50 RDV split [22] for training and evaluation. Inspired by [27], we adopt an unseen-verb setting to evaluate generalization in surgical triplet prediction. Since the original split of [27] is not publicly available, we construct our own unseen-verb subset under the RDV split by removing all training frames containing the verbs *irrigate*, *retract*, *pack*, and *aspirate*, and evaluating on triplets involving these verbs. Additionally, under the RDV split, we analyze performance on uncommon instrument-verb pairs by grouping all triplet classes according to their (instrument, verb) pairs and reporting the mean AP within each group.

c) *Embedding Alignment Visualization*: To analyze fine-grained visual-text alignment, we visualize cosine similarity heatmaps between visual tokens and triplet text embeddings. Since V-JEPA2 uses a temporal stride of 2, tokens from every two consecutive frames are grouped into one temporal unit. After the predictor, cosine similarity between each output token and the triplet text embedding produces one similarity map per unit. Each heatmap is overlaid on the second frame of the pair and bilinearly upsampled to the original resolution.

C. Implementation and Training Details

We follow the two-stage training strategy of VL-JEPA [2], on TrajPred In the first stage, the model is trained

without trajectory tokens to establish basic visual-language alignment, and in the second stage full model is trained with video clips. ALL video clips used for baseline and TrajPred are constructed by augmenting each frame with six preceding frames. All training are done by using 3 RTX Pro 6000 Blackwell GPUs. The text encoder is updated via prompt tuning only with 4 context learnable tokens, and the visual encoder remains frozen. We use AdamW with learning rates of 5×10^{-5} (predictor), 1×10^{-4} (trajectory modules), and 2.5×10^{-6} (text encoder). Finally, we use V-jepa2 [1] as the visual encoder and initialize the predictor with last 8 layers of llama3.2-1B.

D. Demo Video

CholecT50 is derived from CholecT80 [29] by sampling frames at 1 FPS. Accordingly, we train and evaluate under the same 1-FPS RDV split for fair comparison. To examine robustness at higher temporal resolution, we additionally provide a demo on an overlapping Cholec80 clip with available ground-truth triplets. In this demo, frames are sampled at 10 FPS using a six-frame sliding window, and heatmaps are generated from the top-1 prediction.

E. Results

1) *RDV Data Splitting and Unseen Verb Results*: Table II reports AP and Top@K results under the RDV split and unseen-verb setting to show the overall performance of TrajPred. Our TrajPred consistently outperforms all baselines across all metrics. Under RDV, it achieves the best AP_I (86.37), AP_V (59.23), AP_T (36.01), and AP_{IVT} (14.77), as well as the highest $\text{Top@}(K=|\text{GT}|)$ (65.45) and Top@20 (97.02). Table IV further shows that incorporating trajectory information improves recognition of all uncommon triplets, notably “grasper-pack” and “bipolar-grasp”. In the unseen-verb setting, TrajPred maintains clear gains, reaching AP_{IVT} of 11.26 and the highest $\text{Top@}(K=|\text{GT}|)$ score, demonstrating stronger generalization to unseen verb compositions. Table V also shows consistent per-class AP improvements, particularly for motion-intensive interactions such as tool retraction and fluid aspiration. Table IV shows that TrajPred also achieves gains on less frequent instrument-verb pairs. For example, performance improves from 18.1 to 32.9 for Grasper-pack (+14.8), from 0.2 to 0.8 for Grasper-dissect (+0.6), and from 2.8 to 4.2 for Bipolar-retract (+1.4), demonstrating stronger modeling of uncommon actions.

2) *Ablation Study*: Table III reports an ablation study of verb rephrasing and trajectory-token conditioning, evaluating the proposed modules built on top of VL-JEPA. Under the Standard RDV setting, trajectory tokens improve $\text{TOP@}(K=|\text{GT}|)$ from 60.51 to 65.37, while verb rephrasing provides a smaller gain (60.23). The full model achieves the best result of 65.45. Similar improvements are observed in the Unseen-Verb setting, where the full model reaches 20.88.

3) *Visual features-Text Comparison Results*: We report visualization heatmaps of cosine similarity between visual features and text embeddings to show that TrajPred

TABLE II

OVERALL AVERAGE PRECISION (AP) AND TOP@K=|GT| UNDER RDV [22] SPLIT AND UNSEEN-VERB SETTINGS. ‡ REPRESENTS SURGICAL PRETRAINED VLMS.

Setting	Method	AP _I	AP _V	AP _T	AP _{IVT}	TOP@($K= GT $)	TOP@5	TOP@10	TOP@20
Standard RDV	CLIP-VIT-L-Patch14-FT	73.63	44.43	31.67	12.62	59.32	80.32	87.04	89.60
	CLIP-VIT-L-Patch14-GOAL-FT	76.04	45.93	32.08	13.15	61.07	80.93	87.99	95.04
	SurgVLP-FT‡	71.18	47.70	33.35	12.68	59.02	81.98	88.72	94.93
	HecVL-FT‡	76.07	50.92	32.09	12.67	58.03	78.80	86.59	93.58
	PeskaVL-FT‡	75.20	48.71	30.29	12.12	57.05	76.76	86.43	93.54
	VL-JEPA (Image)	72.51	49.22	31.58	12.65	60.06	81.58	90.04	95.31
	VL-JEPA (Video)	82.95	55.17	34.16	13.49	61.91	79.86	88.81	94.91
	TrajPred (Ours)	86.37	59.23	36.01	14.77	65.45	84.33	91.61	97.02
Unseen Verb	SurgVLP-FT‡	54.57	35.32	21.96	8.09	15.17	22.98	29.07	33.12
	HecVL-FT‡	60.52	35.27	23.76	8.68	16.69	25.55	30.61	34.15
	PeskaVL-FT‡	57.92	35.79	23.70	8.54	17.73	26.97	31.95	34.91
	VL-JEPA (Image)	53.73	32.04	23.94	8.28	17.53	25.65	32.29	34.85
	VL-JEPA (Video)	62.33	35.97	24.88	9.02	19.39	27.67	32.93	35.21
	TrajPred (Ours)	74.31	43.62	26.33	11.26	20.88	28.14	32.99	36.27

TABLE III

ABLATION STUDY OF TRAJPRED UNDER THE STANDARD RDV AND UNSEEN-VERB SETTINGS. WE REPORT TOP@($K=|GT|$).

Setting	Verb Rephrase	Traj Tokens	TOP@($K= GT $)
Standard RDV	×	×	60.51
	✓	×	60.23
	×	✓	65.37
	✓	✓	65.45
Unseen Verb	×	×	17.89
	✓	×	19.28
	×	✓	19.97
	✓	✓	20.88

TABLE IV

AVERAGE PRECISION (AP) ON TRIPLETS CONTAINING UNCOMMON INSTRUMENT-VERB PAIRS. ‡ DENOTES THE COMMON VERB ASSOCIATED WITH THE CORRESPONDING INSTRUMENT.

Instrument	Verb	Occurrence (%)	VL-JEPA (video)	TrajPred
Bipolar	coagulate‡	71.7	18.0	18.8
	dissect	20.9	0.4	0.9
	grasp	3.1	13.7	14.6
	retract	4.3	2.8	4.2
Grasper	retract‡	80.8	37.8	40.2
	grasp	17.6	14.9	13.6
	dissect	1.2	0.2	0.8
	pack	0.4	18.1	32.9
Hook	aspirate‡	71.8	61.9	63.3
	irrigate	12.6	4.9	5.4
	retract	8.1	4.2	5.2
	dissect	7.6	1.1	1.6

produces representations that better localize action-relevant regions. Fig. 4 compares the prediction performance and heatmap quality between TrajPred and the baseline VL-JEPA (without trajectory tokens). Regions with high similarity indicate where the predictor’s visual tokens are most semantically aligned with the surgical action. With trajectory tokens, the highlighted regions concentrate on the active instrument and its interaction site, suggesting that the predictor learns more precise action representations. Moreover, the ground-truth triplets achieve higher confidence scores within the top-5 predictions (e.g., “grasper retract gallbladder” 0.295

TABLE V

PER-CLASS AVERAGE PRECISION (AP) ON SIX SELECTED TRIPLETS CONTAINING UNSEEN VERBS.

Triplet	HecVL-FT	PeskaVLP-FT	TrajPred
“grasper pack gallbladder”	0.39	0.61	1.02
“grasper retract gut”	4.79	3.82	8.40
“grasper retract liver”	28.81	26.35	38.17
“grasper retract omentum”	16.84	14.26	27.18
“irrigator aspirate fluid”	12.22	14.22	22.49
“irrigator irrigate cystic_pedicle”	0.54	0.92	3.05

and “bipolar coagulate cystic-duct” 0.215). In contrast, without trajectory tokens, the heatmaps become diffuse and often shift toward endoscope boundaries, likely reflecting camera motion or background patterns rather than meaningful interactions. Correspondingly, the ground-truth confidence scores drop significantly (0.112 and 0.012). Notably, both triplet heatmaps highlight the two instruments in the scene, which we attribute to the unmasked self-attention in the predictor that enables bidirectional interactions among triplet tokens.

V. DISCUSSION AND FUTURE WORK

The main contribution for verb rephrasing technique mainly lies on the unseen verb setting. Verb rephrasing technique improves overall performance in the Unseen-Verb setting, as shown in Table III. The triplet “grasper pack gallbladder” exhibits very low performance across all models because it is an extremely long-tailed action (Table V). Even in this case, verb rephrasing still provides a small performance improvement. This suggests that alternative linguistic expressions help the model associate unseen contexts with semantically related textual descriptions learned during training. Such an approach can be particularly useful in the surgical domain, where many terms are specialized and less common compared to general-domain vocabulary.

In Table IV, we report the AP scores for triplets where each instrument performs both its common and uncommon

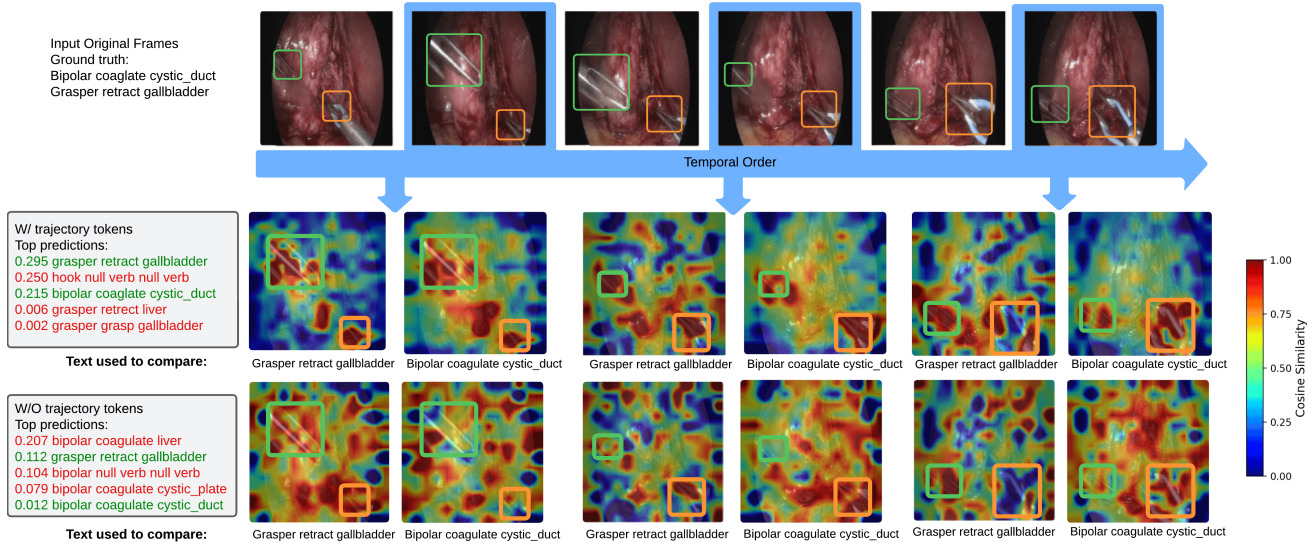


Fig. 4. Image-text similarity heatmaps over six consecutive frames, where red indicates higher cosine similarity. Similarity is computed between predictor-generated spatiotemporal tubelet tokens and the embedding of the ground-truth triplet (when it appears in the top-5 predictions). Each heatmap represents a two-frame temporal unit and is overlaid on the second frame. Top-5 triplet scores are shown alongside the heatmaps. Green and orange bounding boxes denote the grasper and bipolar instruments, respectively.

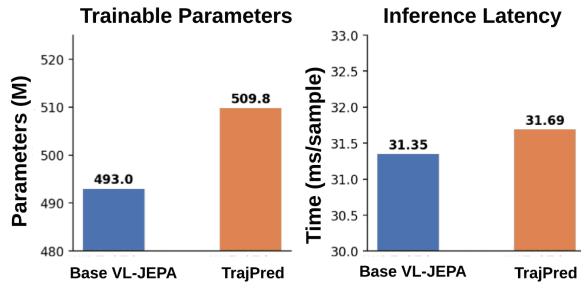


Fig. 5. Comparison of parameter count and inference latency

actions to examine whether trajectory information helps distinguish different instrument behaviors, as instruments may perform multiple actions. Notably, incorporating trajectory information enables TrajPred to achieve improvements on these rare triplets. This suggests that explicitly encoding instrument trajectories helps capture finer details of instrument behavior.

In terms of efficiency, the trajectory token module in TrajPred introduces minimal computational overhead. (Fig. 5). It increases model size by only 3.4 (493.0M \rightarrow 509.8M) and adds at most four trajectory tokens during inference, resulting in negligible extra self-attention cost. End-to-end latency rises by just 0.34 ms per sample (31.35 \rightarrow 31.69 ms, +1.1%). This demonstrates that our trajectory tokens encoding path provides improvement without adding much computational burden.

Finally, we use 1 FPS sampling to capture meaningful motion while reducing redundancy. However, surgical actions vary widely in speed—from rapid cutting to subtle tissue retraction—fixed frame sampling may fail to capture reliable motion cues for all action type; future work will explore adaptive frame rates and extend this spatiotemporal encoding strategy to large-scale pretraining for improved robustness and generalization.

VI. CONCLUSION

In this work, we introduce TrajPred, a predictive embedding framework for surgical VLMs conditioned on instrument trajectory information for surgical action recognition. To address the limited use of temporal information across frames, TrajPred leverages video clips and incorporates trajectory tokens to explicitly encode instrument motion. This trajectory-conditioned prediction further mitigates the loss of fine-grained details often caused by contrastive learning alignment. Experimental results and qualitative visualizations demonstrate improved performance and stronger alignment between image patches and textual representations. These findings highlight the importance of modeling detailed motion cues beyond high-level image- or clip-level vision-language alignment for surgical understanding.

REFERENCES

- [1] Mido Assran, Adrien Bardes, David Fan, Quentin Garrido, Russell Howes, Matthew Muckley, Ammar Rizvi, Claire Roberts, Koustuv Sinha, Artem Zhohus, et al. V-jepa 2: Self-supervised video models enable understanding, prediction and planning. *arXiv preprint arXiv:2506.09985*, 2025.
- [2] Delong Chen, Mustafa Shukor, Theo Moutakanni, Willy Chung, Jade Yu, Tejaswi Kasarla, Allen Bolourchi, Yann LeCun, and Pascale Fung. VI-jepa: Joint embedding predictive architecture for vision-language. *arXiv preprint arXiv:2512.10942*, 2025.
- [3] Hong-You Chen, Zhengfeng Lai, Haotian Zhang, Xinze Wang, Marcin Eichner, Keen You, Meng Cao, Bowen Zhang, Yinfei Yang, and Zhe Gan. Contrastive localized language-image pre-training. *arXiv preprint arXiv:2410.02746*, 2024.
- [4] Xiwen Chen, Wenhui Zhu, Peijie Qiu, Hao Wang, Huayu Li, Haiyu Wu, Aristeidis Sotiras, Yalin Wang, and Abolfazl Razi. Promptot: An optimal transport regularization paradigm for knowledge preservation in vision-language model adaptation. *arXiv preprint arXiv:2503.08906*, 2025.
- [5] Jiajun Cheng, Xianwu Zhao, Sainan Liu, Xiaofan Yu, Ravi Prakash, Patrick J Codd, Jonathan Elliott Katz, and Shan Lin. Surgxbench: Explainable vision-language model benchmark for surgery. *arXiv preprint arXiv:2505.10764*, 2025.

- [6] Hyungyu Choi, Young Kyun Jang, and Chanho Eom. Goal: Global-local object alignment learning. In *Proceedings of the IEEE/CVF Conference on Computer Vision and Pattern Recognition*, pages 4070–4079, 2025.
- [7] Dima Damen, Hazel Doughty, Giovanni Maria Farinella, Sanja Fidler, Antonino Furnari, Evangelos Kazakos, Davide Moltisanti, Jonathan Munro, Toby Perrett, Will Price, et al. Scaling egocentric vision: The epic-kitchens dataset. In *Proceedings of the European conference on computer vision (ECCV)*, pages 720–736, 2018.
- [8] Pierre E Dupont, Bradley J Nelson, Michael Goldfarb, Blake Hannaford, Arianna Menciassi, Marcia K O'Malley, Nabil Simaan, Pietro Valdastri, and Guang-Zhong Yang. A decade retrospective of medical robotics research from 2010 to 2020. *Science robotics*, 6(60):eabi8017, 2021.
- [9] Zheng Fang, Xiaoming Qi, Chun-Mei Feng, Jialun Pei, Weixin Si, and Yueming Jin. Spatio-temporal representation decoupling and enhancement for federated instrument segmentation in surgical videos. *IEEE Transactions on Medical Imaging*, 2026.
- [10] Xiaojie Gao, Yueming Jin, Yonghao Long, Qi Dou, and Pheng-Ann Heng. Trans-svnet: Accurate phase recognition from surgical videos via hybrid embedding aggregation transformer. In *International conference on medical image computing and computer-assisted intervention*, pages 593–603. Springer, 2021.
- [11] Shuangchun Gui and Zhenkun Wang. Tail-enhanced representation learning for surgical triplet recognition. In *International Conference on Medical Image Computing and Computer-Assisted Intervention*, pages 689–699. Springer, 2024.
- [12] Mohammadmahdi Honarmand, Muhammad Abdullah Jamal, and Omid Mohareri. Vidlpro: A video-language pre-training framework for robotic and laparoscopic surgery. *arXiv preprint arXiv:2409.04732*, 2024.
- [13] Amy Jin, Serena Yeung, Jeffrey Jopling, Jonathan Krause, Dan Azagury, Arnold Milstein, and Li Fei-Fei. Tool detection and operative skill assessment in surgical videos using region-based convolutional neural networks. *IEEE Winter Conference on Applications of Computer Vision*, 2018.
- [14] Aishwarya Kamath, Mannat Singh, Yann LeCun, Gabriel Synnaeve, Ishan Misra, and Nicolas Carion. Mdetr-modulated detection for end-to-end multi-modal understanding. In *Proceedings of the IEEE/CVF international conference on computer vision*, pages 1780–1790, 2021.
- [15] Junnan Li, Dongxu Li, Caiming Xiong, and Steven CH Hoi. Blip: Bootstrapping language-image pre-training for unified vision-language understanding and generation. In *International Conference on Machine Learning (ICML)*, 2022.
- [16] Yaoqian Li, Xikai Yang, Dunyuan Xu, Yang Yu, Litao Zhao, Xiaowei Hu, Jinpeng Li, and Pheng-Ann Heng. Surgpub-video: A comprehensive surgical video dataset for enhanced surgical intelligence in vision-language model. *arXiv preprint arXiv:2508.10054*, 2025.
- [17] Shuang Liang, Wentao Ma, and Chi Xie. Relation with free objects for action recognition. *ACM Transactions on Multimedia Computing, Communications and Applications*, 20(2):1–19, 2023.
- [18] Shan Lin, Fangbo Qin, Haonan Peng, Randall A Bly, Kris S Moe, and Blake Hannaford. Multi-frame feature aggregation for real-time instrument segmentation in endoscopic video. *IEEE Robotics and Automation Letters*, 6(4):6773–6780, 2021.
- [19] Daochang Liu, Axel Hu, Mubarak Shah, and Chang Xu. Surgical triplet recognition via diffusion model. *arXiv preprint arXiv:2406.13210*, 2024.
- [20] Yang Liu, Maxence Boels, Luis C Garcia-Peraza-Herrera, Tom Vercauteren, Prokar Dasgupta, Alejandro Granados, and Sebastien Ourselin. Lovit: Long video transformer for surgical phase recognition. *Medical Image Analysis*, 99:103366, 2025.
- [21] C. I. Nwoye, T. Yu, C. Gonzalez, B. Seeliger, P. Mascagni, D. Mutter, J. Marescaux, and N. Padoy. Rendezvous: Attention mechanisms for the recognition of surgical action triplets in endoscopic videos. *Medical Image Analysis*, 78:102433, 2022.
- [22] Chinedu Innocent Nwoye and Nicolas Padoy. Data splits and metrics for method benchmarking on surgical action triplet datasets. *arXiv preprint arXiv:2204.05235*, 2022.
- [23] Alejandra Perez, Chinedu Nwoye, Ramtin Raji Kermani, Omid Mohareri, and Muhammad Abdullah Jamal. Surglavi: Large-scale hierarchical dataset for surgical vision-language representation learning. *arXiv preprint arXiv:2509.10555*, 2025.
- [24] Alec Radford, Jong Wook Kim, Chris Hallacy, Aditya Ramesh, Gabriel Goh, Sandhini Agarwal, Girish Sastry, Amanda Askell, Pamela Mishkin, Jack Clark, et al. Learning transferable visual models from natural language supervision. In *Proceedings of the 38th International Conference on Machine Learning (ICML)*, 2021.
- [25] Anita Rau, Mark Endo, Josiah Aklilu, Jaewoo Heo, Khaled Saab, Alberto Paderno, Jeffrey Jopling, F Christopher Holsinger, and Serena Yeung-Levy. Systematic evaluation of large vision-language models for surgical artificial intelligence. *arXiv preprint arXiv:2504.02799*, 2025.
- [26] Samuel Schmidgall, Justin D Opfermann, Ji Woong Kim, and Axel Krieger. Will your next surgeon be a robot? autonomy and ai in robotic surgery. *Science robotics*, 10(104):eadt0187, 2025.
- [27] Saurav Sharma, Didier Mutter, and Nicolas Padoy. fine-clip: Enhancing zero-shot fine-grained surgical action recognition with vision-language models. *arXiv preprint arXiv:2503.19670*, 2025.
- [28] Saurav Sharma, Chinedu Innocent Nwoye, Didier Mutter, and Nicolas Padoy. Rendezvous in time: an attention-based temporal fusion approach for surgical triplet recognition. *International journal of computer assisted radiology and surgery*, 18(6):1053–1059, 2023.
- [29] Apolline Sauzéon Twinanda, Sherif Shehata, Didier Mutter, Jacques Marescaux, Michel de Mathelin, and Nicolas Padoy. Endonet: A deep architecture for recognition tasks on laparoscopic videos. *IEEE Transactions on Medical Imaging*, 36(1):86–97, 2016.
- [30] Henrique Schechter Vera, Sahil Dua, Biao Zhang, Daniel Salz, Ryan Mullins, Sindhu Raghuram Panyam, Sara Smoot, Iftekhar Naim, Joe Zou, Feiyang Chen, et al. Embeddinggemma: Powerful and lightweight text representations. *arXiv preprint arXiv:2509.20354*, 2025.
- [31] Guankun Wang, Wenjin Mo, Junyi Wang, Long Bai, Kun Yuan, Ming Hu, Jinlin Wu, Junjun He, Yiming Huang, Nicolas Padoy, et al. Surgvidlm: Towards multi-grained surgical video understanding with large language model. *arXiv preprint arXiv:2506.17873*, 2025.
- [32] Zhenhailong Wang, Ansel Blume, Sha Li, Genglin Liu, Jaemin Cho, Zineng Tang, Mohit Bansal, and Heng Ji. Paxion: Patching action knowledge in video-language foundation models. *Advances in Neural Information Processing Systems*, 36:20729–20749, 2023.
- [33] Jiarui Xu, Shalini De Mello, Sifei Liu, Wonmin Byeon, Thomas Breuel, Jan Kautz, and Xiaolong Wang. Groupvit: Semantic segmentation emerges from text supervision. In *Proceedings of the IEEE/CVF conference on computer vision and pattern recognition*, pages 18134–18144, 2022.
- [34] Lewei Yao, Runhui Huang, Lu Hou, Guansong Lu, Minzhe Niu, Hang Xu, Xiaodan Liang, Zhenguang Li, Xin Jiang, and Chunjing Xu. Filip: Fine-grained interactive language-image pre-training. *arXiv preprint arXiv:2111.07783*, 2021.
- [35] Michael Yip. The robot will see you now: Foundation models are the path forward for autonomous robotic surgery. *Science Robotics*, 10(104):eadt0684, 2025.
- [36] Kun Yuan, Vinkle Srivastav, Nassir Navab, and Nicolas Padoy. Hecvl: Hierarchical video-language pretraining for zero-shot surgical phase recognition. *arXiv preprint arXiv:2405.10075*, 2024.
- [37] Kun Yuan, Vinkle Srivastav, Nassir Navab, and Nicolas Padoy. Procedure-aware surgical video-language pretraining with hierarchical knowledge augmentation. In *Proceedings of the 38th Conference on Neural Information Processing Systems (NeurIPS)*, 2024.
- [38] Kun Yuan, Vinkle Srivastav, Tong Yu, Joël L. Lavanchy, Jacques Marescaux, Pietro Mascagni, Nassir Navab, and Nicolas Padoy. Learning multi-modal representations by watching hundreds of surgical video lectures. *arXiv preprint arXiv:2307.15220*, 2023.
- [39] Yan Zeng, Xinsong Zhang, and Hang Li. Multi-grained vision language pre-training: Aligning texts with visual concepts. *arXiv preprint arXiv:2111.08276*, 2021.
- [40] Zhitao Zeng, Zhu Zhuo, Xiaojun Jia, Erli Zhang, Junde Wu, Jiaan Zhang, Yuxuan Wang, Chang Han Low, Jian Jiang, Zilong Zheng, et al. Surgvlm: A large vision-language model and systematic evaluation benchmark for surgical intelligence. *arXiv preprint arXiv:2506.02555*, 2025.
- [41] Chenhao Zheng, Jieyu Zhang, Mohammadreza Salehi, Ziqi Gao, Vishnu Iyengar, Norimasa Kobori, Quan Kong, and Ranjay Krishna. One trajectory, one token: Grounded video tokenization via panoptic sub-object trajectory. In *Proceedings of the IEEE/CVF International Conference on Computer Vision*, pages 23156–23166, 2025.
- [42] Kaiyang Zhou, Jingkang Yang, Chen Change Loy, and Ziwei Liu. Conditional prompt learning for vision-language models. In *Proceedings of the IEEE/CVF Conference on Computer Vision and Pattern Recognition*, pages 16816–16825, 2022.

- [43] Kaiyang Zhou, Jingkang Yang, Chen Change Loy, and Ziwei Liu. Learning to prompt for vision-language models. *International journal of computer vision*, 130(9):2337–2348, 2022.
- [44] Fatimah Zohra, Chen Zhao, Hani Itani, and Bernard Ghanem. beta-clip: Text-conditioned contrastive learning for multi-granular vision-language alignment. *arXiv preprint arXiv:2512.12678*, 2025.